Challenges in measuring low concentration of overlapping elements with EDS and the need for verification with secondary standard composition

Lucia Spasevski*, *Philippe T.* Pinard, *John Qing* Zhang *and Simon* Burgess

Oxford Instruments NanoAnalysis, Halifax Road, High Wycombe, HP12 3SE, United Kingdom

Abstract. Quantitative analysis using energy-dispersive spectrometry (EDS) has been shown to achieve high accuracy equivalent to that of wavelength-dispersive x-ray spectrometry (WDS) even in the case of highly overlapped X-ray peaks of major elements and high precision in the case of trace elements with concentrations below 1 wt.%. With reliable pulse pile-up correction, accurate, unnormalized EDS quantification was also demonstrated at count rates above 200 kcps. This work studies the EDS quantification of samples exhibiting these three analytical challenges simultaneously: quantification of trace elements (< 1 wt%), overlapping X-ray peaks of major elements (small peak on large peak), and high-count rates (to improve productivity of these measurements). A secondary standard was used to optimise and validate the collection conditions for the measurement of an unknown slag sample exhibiting a heterogeneous microstructure containing trace level of Mn. Accurate quantification down to 0.1 wt% and mapping of segregation in the order of 0.2wt% were possible with modern EDS technology.

1 Introduction

Energy-dispersive X-ray spectrometry (EDS) is being used with increasing frequency to obtain materials compositional information. Improvements to silicon drift detector (SDD) technology and careful characterisation of EDS parameters have improved the accuracy and sensitivity of quantitative analyses [1]. For instance, Newbury and Ritchie [2] achieved relative errors of less than 1% on the mass fractions obtained by EDS quantification of PbS, MoS_2, $BaTiO_3$, $SrWO_4$ and WSi_2; all compounds with major elements (> 10 wt%) with X-ray peaks with a separation of less than 40 eV. While EDS has a worse spectral resolution than WDS, deconvolution of EDS X-ray peaks can reproduce similar level of accuracy as WDS measurements.

The detection and quantification of minor (1 – 10 wt%) and trace (< 1 wt%) elements is a strength of WDS analysis. The better spectral resolution of WDS translates into higher P/B ratios and lower detection limits. The spectral resolution also avoids issues of interfering X-ray peaks in most cases. The diffracting crystal acts as a filter, filtering out the large number of X-rays emitted from major elements, only collecting X-rays from the low concentration elements, at the selected Bragg diffraction angle. This allows high beam currents to be used without saturating the spectrometers, and therefore good counting statistics can be achieved within an acceptable measurement time. However, WDS analysis has some downsides. The electron dose that a sample can sustain without damage is not infinite, nor is the maximum beam current realistically achievable by an electron microscope. The spatial resolution of scanning electron microscopes (SEM) and electron microprobes deteriorates with increasing beam currents [11]. At large beam currents, the beam diameter becomes an important factor influencing the interaction volume, limiting the ability to measure small features containing low concentration elements. Most SEMs are also limited to a beam current of 40-50 nA. Modern large area EDS-SDDs, with their large solid angles [4], are therefore more suited to work under the typical beam currents used in SEMs (1 – 20 nA).

Despite lower P/B ratios and worse spectral resolution, EDS has been shown to achieve high accuracy equivalent to that of WDS even in the cases of minor and trace elements with severe interference from a major element [2-3]. For example, Newbury and Ritchie [2] studied a glass standard K2496 containing Ba (major concentration of 42.99 wt%) and Ti (minor concentration of 1.8 wt%) and obtained a relative error of 2.4% for Ti; as for $BaTiO_3$ the deconvolution of Ba L and Ti K X-ray peaks is required for the accurate quantification. The

* Corresponding author: lucia.spasevski@oxinst.com

© The Authors, published by EDP Sciences. This is an open access article distributed under the terms of the Creative Commons Attribution License 4.0 (https://creativecommons.org/licenses/by/4.0/).

small relative error demonstrates the deconvolution of EDS X-ray peaks is possible even if one of the deconvolved X-ray series has a much lower intensity than the other. By acquiring spectra with 120 million counts, they detected the presence of 0.41 wt%Ta (overlapping with 11.5 wt%Si) and 0.41 wt%Ce (overlapping with 21.94 wt%Ba) in the K873 glass standard but obtained a worse quantification accuracy (~25%) than with major and minor element interferences [3]. The authors operated their EDS detectors with a time constant yielding a Mn Kα resolution of 128.5 eV and a dead time of ~10%, resulting in a low output count rate and long measurement time.
With modern electronics, pulse processors and pulse pile-up correction algorithms, EDS-SDDs can operate at high count rates in the hundred thousand of cps [4]. Pinard et al. [5] measured 53 standard samples containing mostly major elements at an input count rate of 50 kcps and 200 kcps. The quantification was performed using a remote-standard standardless approach and a single beam calibration on Co to achieve unnormalized results. The quantification was performed using a remote-standard standardless approach, which relies on a database of X-ray intensities acquired at the factory on different standards and a correction for the difference in detector efficiency between the current and gold standard detector (see [5] for more details). A single beam calibration on Co was also performed to achieve unnormalized results.

At both count rates, the authors achieved a relative error of less than 5%, demonstrating the stability of the spectrometer at different count rates as well as the accuracy of the standardless approach, peak deconvolution and pulse pile-up correction.

Building on the aforementioned publications, the challenge put forward in this work is to evaluate EDS quantification of trace elements whose X-ray peaks are severely overlapped by X-ray peaks of major elements at high count rates, with the aim of improving the productivity of these measurements in the SEM. This work was initiated from the analysis of a furnace slag sample with a heterogenous microstructure, including a particular phase containing trace levels of Mn. In order to establish and validate the acquisition procedure, a standard alloy sample with similar elemental content and analytical challenges to the unknown slag was used. The unknown slag sample was then investigated by performing WDS and EDS mapping at high count rate conditions, and the results compared across the different techniques.

2 Materials and methods

The sample of interest in this work is the slag sample obtained from the experimental work in a steel production furnace. The heterogeneous microstructure contains various major elements (**Figure 1**) and trace elements like Na, P, S, K, Ca, Ti, V and Mn. The latter has been detected in the Cr-rich region (**Figure 1**f), which poses a particular challenge to measure with EDS due to the overlap between Mn-Kα (5.899 keV) and Cr-Kβ (5.947 keV), a 48 eV separation. The measurement is further complicated due to sum peaks from other X-ray lines piling up on top of the overlapping Cr-Kβ / Mn-Kα peak, notably Cr-Kα + O-Kα (5.941 keV), Cr-Kα + Cr-Lα (5.988 keV) and Cr-Kα + Cr-Lℓ (5.915 keV). The quantification of Mn is therefore only possible with an accurate pulse pile-up correction and peak deconvolution.

Finding well-defined standards to validate analysis containing minor and trace elements with overlapping X-ray peaks was found to be challenging. A standard reference material, XPE16 [7], was identified as the best available suitable secondary standard due to its similar element content to unknown slag sample (nominal composition shown in **Table 1** and due to similar X-ray line overlaps. It contains a similar trace level of Mn (~0.05 wt%) and a large concentration of Cr (17 wt%) which allows the validation of the pulse pile-up correction of Cr sum peaks and peak deconvolution of Mn and Cr.

The materials were analysed using EDS (Ultim Max Infinity 65, Oxford Instruments, United Kingdom) and WDS (AZtec Wave, Oxford Instruments, United Kingdom) on a Hitachi SU70 SEM (Hitachi High Tech, Japan). The EDS detector utilises the TruQ-IQ technology where each detector is individually characterised during manufacturing to refine the collection and processing parameters [8], notably the pulse pile-up correction which is of particular relevance to this work. On the XPE16 standard, WDS measurements were acquired at 20 kV, 4 nA using the LiF crystal with a peak time of 70 s and background time of 50 s, background positions were 6.16683 and 5.6336 keV, standard used for Mn was pure Mn. EDS was acquired during the whole WDS acquisition, with input count rate of 115 kcps and quantification of all other elements was performed using a standardless approach. Optimisation of EDS collection conditions was also performed using the XPE16 standard. EDS spectra at different process times and input count rates were acquired with a count limit of 25 million counts. Finally, a combined EDS-WDS map was acquired at 20 kV, 20 nA over a region of interest on the unknown slag sample, using the WDS LiF-crystal and an EDS input count rate of 500 kcps, process time 3 for 174 min.

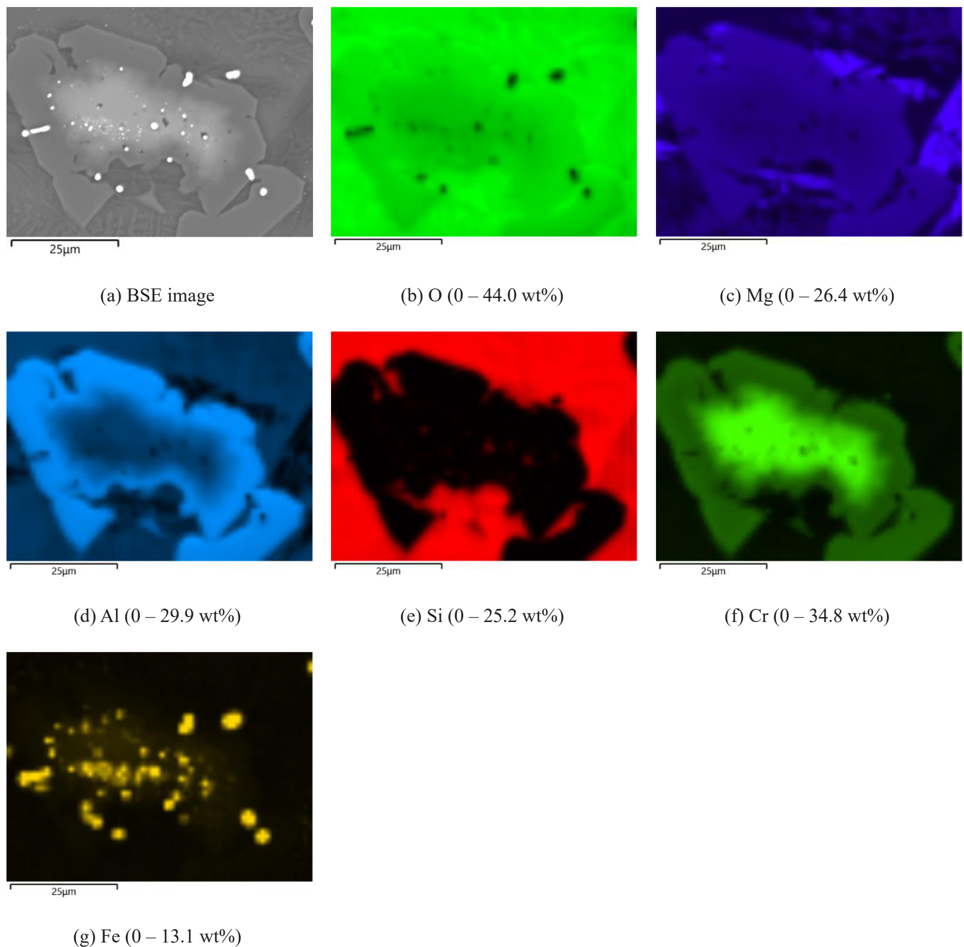

(a) BSE image (b) O (0 – 44.0 wt%) (c) Mg (0 – 26.4 wt%)

(d) Al (0 – 29.9 wt%) (e) Si (0 – 25.2 wt%) (f) Cr (0 – 34.8 wt%)

(g) Fe (0 – 13.1 wt%)

Figure 1. (a) Backscattered electron (BSE) image of a representative area of the furnace slag sample, (b-g) quantitative elemental maps showing the distribution of the major elements. The wt% range used in the respective colour scale of each map is shown in parenthesis.

3 Experimental results

3.1 Reference WDS/EDS quantitative analysis on the XPE16 standard

The nominal composition of the XPE16 standard was first measured by WDS/EDS, where Mn was measured by WDS and all other elements were measured by EDS (**Table 1**). WDS measurement of Mn does not suffer from the same EDS difficulties previously mentioned (i.e., strong overlap, and sum peaks) and serves as a reference point when accessing the quality of EDS measurements. The average measured Mn concentration with WDS in XPE16 standard was 0.0947 ± 0.0102 wt%, which differs from the certified concentration of 0.05 wt%, while the measured concentrations of all other elements measured are within the margin of error. This highlights the issue of the availability of suitable standard materials for validating EDS analysis at low concentrations.

Table 1. WDS/EDS reference measurements for XPE16 standard (all values in wt%).

Points	Al	Si	Ti	Cr	Mn	Fe	Co	Ni	Mo	Total
1	1.31	0.15	1.17	17.76	0.1075	34.25	0.15	42.86	3.22	100.99
2	1.30	0.16	1.18	17.69	0.0982	34.03	0.18	42.71	3.27	100.63
3	1.30	0.16	1.47	17.63	0.0870	33.72	0.16	42.49	3.34	100.37
4	1.30	0.15	1.11	17.68	0.0859	34.35	0.19	42.57	3.11	100.54
Average	1.30	0.16	1.23	17.69	0.0947	34.09	0.17	42.66	3.24	100.63
Standard Deviation	0.01	0.01	0.16	0.05	0.0102	0.28	0.02	0.16	0.10	0.01
Nominal	*1.27*	*0.15*	*1.25*	*17.00*	*0.0500*	*33.88*	*0.09*	*42.80*	*3.41*	*99.90*

3.2 Optimisation and validation of EDS quantitative analysis

One potential advantage of the EDS technique is being able to achieve higher throughput / speed with a low beam current compared to WDS, as data from all elements is collected in parallel, and large area detectors offer much higher solid angles. However, at higher count rate EDS suffers from worse spectral resolution and pulse pile-up effects. To study these effects, EDS quantitative results acquired under different conditions were compared against WDS reference values for Mn in the standard XPE16 alloy. Specifically, three parameters were studied: (1) the counting time to achieve the detection limit required to measure a trace level of Mn, (2) the detector shaping time, also known as process time, which influences the throughput and spectral resolution, and (3) the input count rate, which influences the pulse pile-up effects.

3.2.1 Detection limit and counting time

The following equation is often used to evaluate the detection limit of a particular element [3]:

$$C_{DL} = n\left(\frac{\sqrt{n_B}}{n_{std}}\right)C_{std}$$

where n_B and n_{std} correspond to the background counts and net counts measured on a standard containing the element of interest in concentration C_{std}. The factor n can vary from 3 to 10 depending on whether the criterion is used to assess the detectability or threshold for quantitative analysis. Increasing the counting time increases proportionately the background and net counts but the square root of the background counts means that the counting time must be increased by a factor of 4 to improve the detection limit by a factor of 2.

It is however difficult to apply this equation to the detection limit of EDS measurements for two reasons. First, there is no direct measurement of the background intensity. Spectrum processing either uses background filtering or subtraction to extract net intensities of X-ray peaks in a spectrum. The background intensity below an EDS X-ray peak is never directly used. Secondly, the equation does not consider the influence of peak deconvolution (or more generally peak interference). For EDS, least-squares fitting is typically used to deconvolve overlapping X-ray peaks, and the error associated with the deconvolution influences the detection limit [9].

An alternative approach to determine the detection limit for a given counting time is to use spectrum synthesis [10]. A spectrum for any composition can be simulated based on first-principal physics parameters, characteristics of the EDS detector (e.g., detector efficiency, spectral resolution, geometry) and specified collection conditions (e.g., beam voltage, beam current, live time). Poisson counting statistics is then randomly applied to the spectrum. The spectrum can then be quantified using the exact same spectrum processing routine as real experimental

spectra. The calculated uncertainty on the weight fraction reported in the quantification results combines the counting statistics uncertainty and the error in the spectrum processing. The detection limit of any element corresponds to the uncertainty multiplied by 3 to obtain the significant sigma limit.

Using the measured concentration of XPE16 standard (**Table 1**), spectra were synthesised using the same acquisition conditions but increasing live times. Examples of two synthesised spectra with 200,000 and 25 million counts are shown in **Figure 2** alongside a spectrum without Mn. The small difference between the spectrum with and without Mn illustrates the need of collecting high count spectra to detect and quantify Mn. **Figure 3** shows the calculated detection limit as a function of total number of counts in the spectrum, as well as the detection limit of two experimental spectra acquired with 2 and 25 million counts. Spectrum synthesis slightly overestimates the detection limit but matches the experimental trend as a function of total spectrum area. Based on this analysis, it was established that a 25 million count limit gives adequate detection limit (~0.012wt% or 120 ppm) for a trace level of Mn in high Cr containing samples.

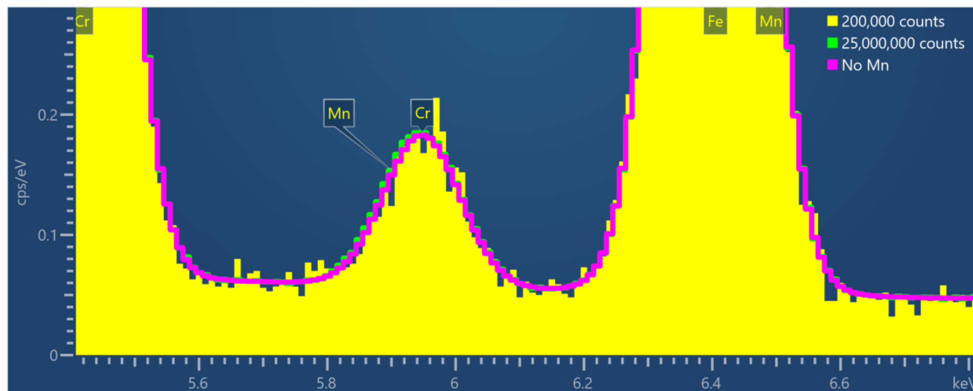

Figure 2. Comparison of synthesised spectrum of XPE16 standard with different total spectrum areas (200,000 and 25 million counts) as well as a synthesised spectra without Mn.

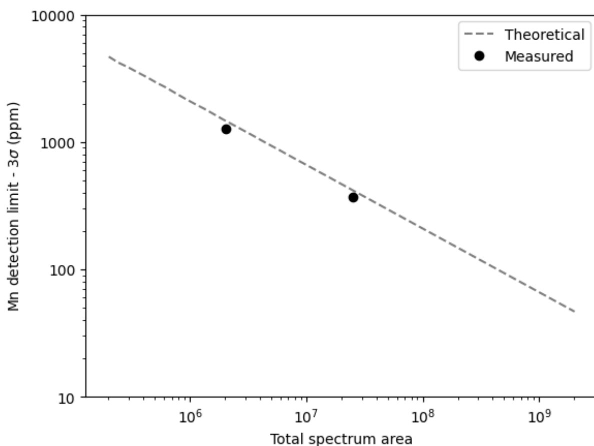

Figure 3. Investigation of the required total spectrum area to determine the detection limit of Mn in the XPE16 standard using synthesised spectra. The two dots on the plot represent the detection limit determined from experimental spectra acquired with 2 and 25 million total spectrum area.

3.2.2 Process time

Figure **4** shows the Mn concentrations measured in XPE16 standard at different process times (PT). The input count rate was kept constant at 200 kcps and all spectra were acquired with a total spectrum area of 25 million counts. All elements were quantified by EDS using a remote-standard standardless approach and a single beam calibration on Co to achieve unnormalized results. The error bars correspond to the 1-sigma uncertainty. The dash

lines correspond to the 1-sigma uncertainty around the measured Mn concentration by WDS. Longer process time means longer pulse processing time and better spectral resolution. For this detector, the spectral resolution measured as the FWHM of Mn Kα X-ray peak varies between 146 and 124 eV for PT2 and 5, respectively. There is good agreement between the EDS and WDS Mn concentrations for PT3, 4 and 5. More investigation is needed to understand the measured Mn concentration at PT2. A possible explanation might be the resolution degradation which makes the deconvolution of the small Mn X-ray peak from the large Cr X-ray peak more challenging. Based on this set of data it was possible to conclude that the fastest processing time that still provides accurate quantitative results was PT3.

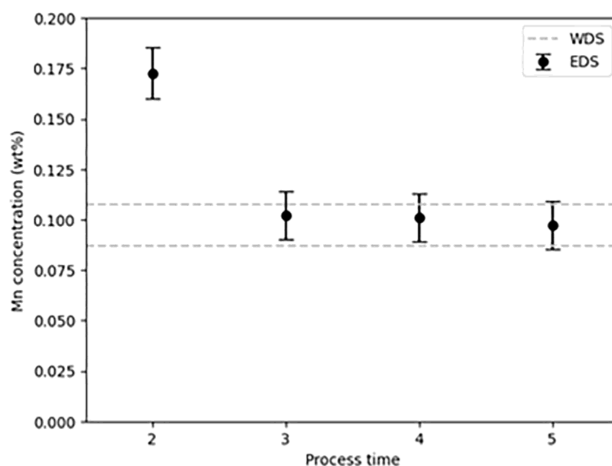

Figure 4. Investigation of the process time influence on the measurement of Mn concentration with the XPE16 standard. PT2 represents shortest shaping time and PT5 longest shaping time.

3.2.3 Input count rates

With increasing input count rates, the pulse pile-up effects become the limiting factor affecting performance. Pulse pile-up events happen when two or more X-ray events cannot be individually distinguished by the pulse processor. The result is a single X-ray event measured with an incorrect energy; its energy being the sum of the individual X-ray events. Sum peaks, the result of two or more characteristic X-ray events, are common potential artefacts in EDS spectra, but pulse pile-ups of characteristic and Bremsstrahlung X-ray events are also significant at high count rates and can influence the shape of the continuum and X-ray peaks. A combination of pulse pile-up suppression by the pulse processor and pulse pile-up correction by the spectrum processing can remove pulse pile-up effects in EDS spectra.

The measurement of Mn in the XPE16 standard is a good test to assess the pulse pile-up correction due to the interference of the Cr-Kα + Cr-Lα (5.988 keV) and Cr-Kα + Cr-Lℓ (5.915 keV) sum peaks with the Mn Kα X-ray peak. Using PT3 and a total spectrum area of 25 million counts, spectra were acquired on XPE16 standard at increasing input count rates from 23 kcps (19 min total acquisition count time) to 800 kcps (90 s total acquisition count time). Figure 5 shows good agreement between EDS and WDS data at all count rates, indicating that the pulse pile-up correction and peak deconvolution has been adequate, meaning the peak intensities have been corrected for all the spectrum artifacts.

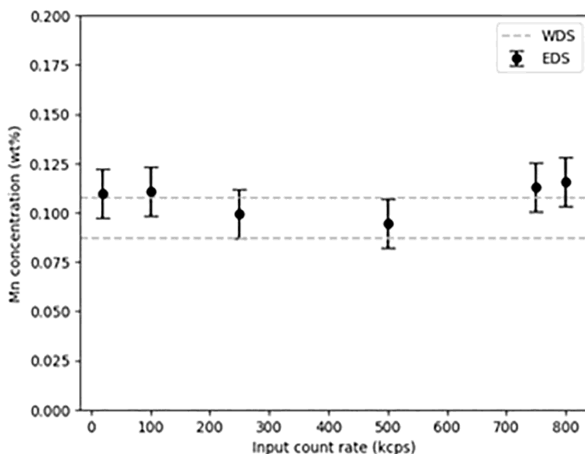

Figure 5. Investigation of the input count rate influence on the measurement of Mn concentration with the XPE16 standard at PT3.

3.3 Blank measurement

A blank measurement involves measuring the concentration of an element of interest in a standard sample that do not contain that element. This is useful to assess the accuracy of low concentration measurements. In this work Mn concentration was also measured using pure Cr and Ni standard samples which are serving as a blank correction estimate (Table 2 and 3). Data was acquired at the same analytical conditions that are used to analyse unknown slag sample (20kV, 20nA, PT3 and an input count rate of 500 kcps). In the case of Cr standard there is also significant overlap between Mn-Kα line position and Cr-Kβ. When measuring Mn in Cr standard serving as "blank measurement" the average measured Mn concentration with EDS was -0.0151 ± 0.0076 wt%.

Table 2. WDS/EDS reference measurements for Cr blank standard (all values in wt%).

Points	Cr	Mn (EDS)
1	99.4912	-0.0066
2	99.7853	-0.0170
3	100.1489	-0.0246
4	100.2029	-0.0123
Average	99.9071	-0.0151
Standard Deviation	0.3335	0.0076
Nominal	100.0000	0.0000

Table 3. WDS/EDS reference measurements for Ni blank standard (all values in wt%).

Points	Ni	Mn (EDS)
1	98.5972	0.0050
2	98.7799	-0.0114
3	98.6170	-0.0055
4	98.2746	-0.0086
Average	98.5672	-0.0051

Standard Deviation	0.2115	0.0072
Nominal	100.0000	0.0000

Another test for blank measurement was performed using pure Ni sample, using same condition as for the pure Cr sample. In this standard there is no overlap between theoretical Mn-Kα line position and Ni-Kα. When measuring Mn in Ni standard serving as "blank measurement" the average measured Mn concentration with EDS was -0.0051 ± 0.0072 wt%. Results are indicating that EDS is not overestimating the Mn concentration, and the values are close to the expected nominal value of 0 wt%.

3.4 WDS/EDS mapping of the unknown slag sample

The unknown furnace slag sample was mapped at 20kV, 20nA using PT3 and an input count rate of 500 kcps (dead time of ~45%) over a representative area. While higher input count rates could be possible based on the results in Figure 5, the input count rate was selected to maintain an acceptable dead time (< 60%) across all the phases in the field of view. Simultaneous EDS and WDS data were collected for 1300 frames, totalling a total acquisition time of 174 min. The original EDS and WDS data (256 x 192) were binned by a factor 4 to improve the counting statistics of each pixel. The BSE image and elemental distribution of the major elements are shown in Figure 1.

Figure 6 shows the WDS and EDS mapping results for Mn. WDS map correspond to the true elemental distribution of Mn within the region of interest, albeit in this instance the Bremsstrahlung contribution was not removed. As WDS does not suffer from the same analytical difficulties as EDS (i.e., strong overlap, and sum peaks), Figure 6a should correspond to the true elemental distribution of Mn within the region of interest. The comparison between Figure 6a and b confirms the peak overlaps with Mn-Kα and Cr-Kβ, as the Mn window integral map matches the Cr map (Figure 1f). Even after performing spectrum processing at every pixel of the map to filter the continuum and deconvolve peaks (Figure 6c) WDS and EDS maps do not display the same information. There is a higher Mn intensity in the middle Cr-rich region than in the periphery phase in the EDS map compared to the WDS map. As explained previously, the reason for this mismatch is the pulse pile-up effects. The pulse pile-up correction was not applied to the pixel spectra to generate Figure 6b and therefore the Mn intensity is artificially inflated by the Cr-Kα + O-Kα, Cr-Kα + Cr-Lα and Cr-Kα + Cr-Lℓ sum peaks. This can be visualised in Figure 7 where a spectrum was reconstructed using the EDS hyperspectral map from the Cr-rich region. The original spectrum without pulse pile-up correction (but including pulse pile-up suppression) in green shows higher counts on the left-hand side of the Cr-Kβ peak than the pulse pile-up corrected spectrum in yellow, matching the expected energies of the sum peaks. Figure 6d shows the final result where the pulse pile-up correction is applied to each pixel spectrum followed by continuum filtering and peak deconvolution. There is a good agreement between the Mn elemental distribution measured by EDS and WDS (Figure 6a). The decrease in the Mn intensity around the Cr-rich region is observed in both maps as well as the presence of Mn in the phase at the periphery of the field of view.

The detection limit of Mn obtained by the EDS mapping can be assessed by extracting pixel spectra from the Cr-rich region. Each pixel spectrum contains around 800,000 total counts, yielding an uncertainty on the Mn concentration around 0.07 wt%. Unnormalized quantitative results from 5 reconstructed spectra are shown in Table 4, give an average Mn concentration of 0.26 wt%.

The ability to extract additional information after the acquisition like quantitative results from reconstructed spectra is a benefit of hyperspectral EDS mapping. Another is to further analyse reconstructed spectra from different phases and identify the presence of a priori unknown elements. In this example, the presence of other trace elements (Na, S, K, Ca, Ti and V) was identified from the map sum spectrum and reconstructed spectra of the respective phases. The quantitative elemental distribution of these elements is shown in Figure 8. The Ti distribution follows the Mn distribution, whereas the V follows the Cr distribution (Figure 1f). Some of the Fe inclusions (Figure 1g) contain S but not all of them. Further investigation is required to understand the relationship between these elemental distributions.

https://doi.org/10.1051/epjconf/202634901016

(a) WDS

(b) EDS-Window integral

(c) EDS-Peak deconvolution

(d) EDS-Pulse pile-up correction and peak deconvolution

Figure 6. WDS and EDS Mn intensity maps collected from the slag sample. Different levels of spectrum processing were applied to the EDS dataset.

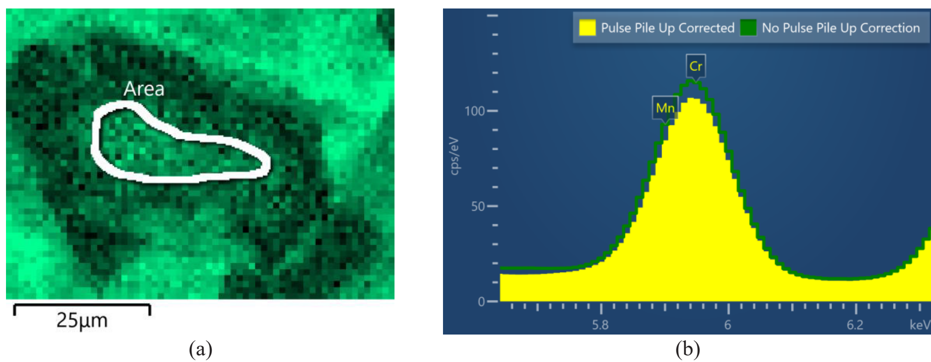

(a) (b)

Figure 7. (a) Cr-rich / Mn area where a spectrum was extracted. (b) Comparison of the original spectrum without pulse pile-up correction (green) and the pulse pile-up corrected spectrum (yellow).

Table 4. EDS measurements from extracted spectra from the Cr-rich region of the slag sample (all values in wt%).

Point	O	Mg	Al	Si	P	Ti	V	Cr	Mn	Fe	Total
1	36.64	12.53	11.52	0.39	0.02	0.39	0.10	35.54	0.23	3.06	100.4
2	36.9	12.61	12.06	0.3	0.01	0.36	0.11	35.04	0.23	3.33	100.96
3	37.11	12.92	12.33	0.29	-0.02	0.38	0.11	35.53	0.31	1.77	100.74
4	36.91	12.99	12.27	0.25	0.02	0.35	0.12	34.86	0.27	2.21	100.24
5	37.17	12.93	12.57	0.2	0.01	0.36	0.17	34.56	0.24	2.94	101.16
Average	36.95	12.79	12.15	0.29	0.01	0.37	0.12	35.1	0.26	2.66	100.70
Std. Dev.	0.21	0.21	0.39	0.07	0.02	0.02	0.03	0.43	0.03	0.65	0.38

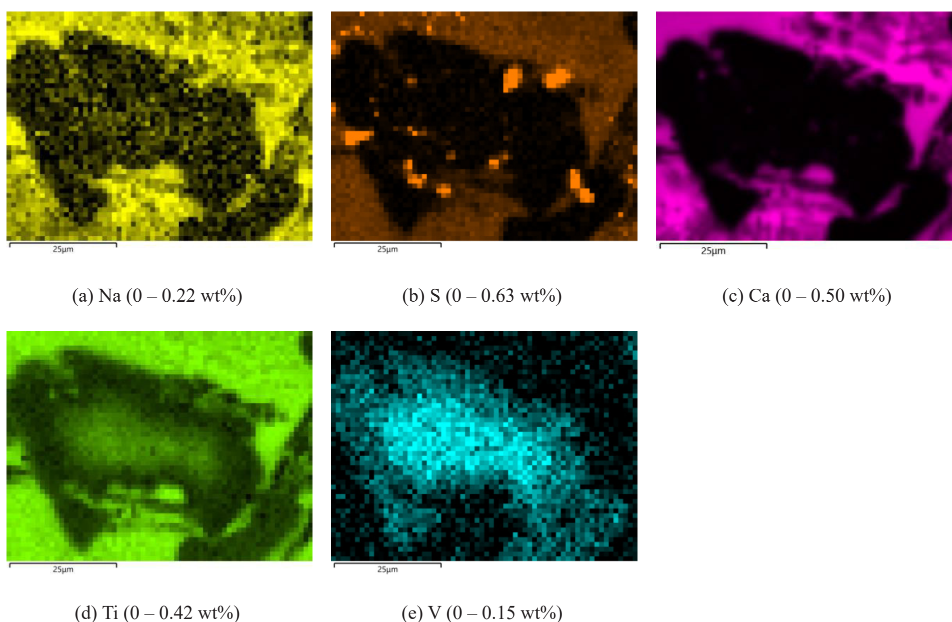

(a) Na (0 – 0.22 wt%) (b) S (0 – 0.63 wt%) (c) Ca (0 – 0.50 wt%)

(d) Ti (0 – 0.42 wt%) (e) V (0 – 0.15 wt%)

Figure 8. Quantitative elemental maps showing the distribution of the trace elements. The wt% range used in the respective colour scale of each map is shown in parenthesis.

4 Conclusion

The tests performed on the furnace slag sample and secondary XPE16 standard give encouraging results that EDS characterisation down to concentration levels of 0.1 wt% at high count rates is possible, even in the case of significant major peak overlaps and pulse pile-up effects. The secondary standard was used to optimise the collection conditions. With large area detectors and their higher solid angle, one potential advantage of EDS for trace element analysis is the ability to use lower beam currents compared to WDS, to achieve higher spatial resolution and characterize smaller features in a sample. The optimised pulse pile-up correction on a per detector basis [8] means that EDS analysis can be acquired at high count rates without affecting the accuracy of the quantification. Processing EDS maps solely to filter out the continuum and deconvolve peak overlaps was not sufficient to reveal the true distribution of Mn in the sample as measured by WDS mapping. The correct elemental distribution was only achieved after pulse pile-up correction, background filtering and peak deconvolution were applied to each pixel spectrum. Results also highlight the need for well-characterised standard materials that can serve as reference samples to optimise and validate challenging analytical situations as well as to assess the quality of different EDS detectors and the accuracy of quantification procedures.

References

1. S Burgess, H James, P Statham, L Xiaobing, Using Windowless EDS Analysis of 45-1000eV X-ray Lines to Extend the Boundaries of EDS Nanoanalysis in the SEM, Microscopy and Microanalysis, **19**, Issue S2, (2013), 1142–1143, https://doi.org/10.1017/S1431927613007708
2. DE Newbury, NW Ritchie, Performing elemental microanalysis with high accuracy and high precision by scanning electron microscopy/silicon drift detector energy-dispersive X-ray spectrometry (SEM/SDD-EDS). J Mater Sci., **50**(2):493-518. (2015), doi: 10.1007/s10853-014-8685-2
3. DE Newbury, NWM Ritchie, Measurement of Trace Constituents by Electron-Excited X-Ray Microanalysis with Energy-Dispersive Spectrometry, Microscopy and Microanalysis, **22**(3), 520–535, (2016) https://doi.org/10.1017/S1431927616000738
4. S Burgess, C Collins, J Holland, N Rowlands, High Speed Accurate Quantification with X-Max Large Area Silicon Drift Detectors, Microscopy and Microanalysis, **16**, Issue S2, 1320–1321, (2010) https://doi.org/10.1017/S143192761005909X
5. P. Pinard, A. Protheroe, J. Holland, S. Burgess, P. Statham, Development and validation of standardless and standards-based X-ray microanalysis. IOP Conference Series: Materials Science and Engineering, **891**. 012020, (2020). 10.1088/1757-899X/891/1/012020.
6. P. Statham, Pile-Up Correction for Improved Accuracy and Speed of X-Ray Analysis. Microchimica Acta. **155**. 289-294 (2006). 10.1007/s00604-006-0558-1.
7. Original scan of the alloy composition sheet (2025), adding URL https://oxinst-my.sharepoint.com/:b:/p/lucia_spasevski/EYZ7mKLy6HBNoitM4S0EfZEBgAn4A-Rs8iP7ZyQVhY-5jQ?e=MvTdNZ
8. P. Pinard, S. Burgess, J. Qing Zhang, PJ. Statham, Characterizat, Ion and Customization of Individual EDS Detectors to Improve X-ray Microanalysis of Light Elements, Microscopy and Microanalysis, **30**, Issue Supplement (2024), ozae044.096, https://doi.org/10.1093/mam/ozae044.096
9. P. Statham, Deconvolution and background subtraction by least-squares fitting with prefiltering of spectra. Analytical Chemistry, **49**, 2149 – 2154 (1977). https://doi.org/10.1021/ac50022a014
10. PJ. Statham, C. Penmen, P. Duncumb, Improved spectrum simulation for validating SEM-EDS analysis, IOP Conference Series: Materials Science and Engineering **109**, 01 (2016). 10.1088/1757-899X/109/1/012016
11. P. Pinard, and S. Richter, Quantification of low concentration elements using soft X-rays at high spatial resolution. IOP Conference Series: Materials Science and Engineering **109**, 012013 (2016). http://dx.doi.org/10.1088/1757-899X/109/1/012013